Est. 1984

ORIENTAL JOURNAL OF CHEMISTRY
An International Open Free Access, Peer Reviewed Research Journal

www.orientjchem.org

ISSN: 0970-020 X
CODEN: OJCHEG
2016, Vol. 32, No. (6):
Pg. 3183-3188

Physico-Chemical Studies of a New Zr-doped $BaBeTiO_3$ System

ABDELHALIM ELBASSET[1,2]*, LAMIAE MRHARRAB[2], SALAHEDDINE SAYOURI[2], FARID ABDI[1] and TAJ-DINE LAMCHARFI[1]

[1]LSSC Department of Electrical Engineering, Faculty of Sciences and Techniques, University Sidi Mohmmed ben Abdelah, Fes, Morocco.
[2]LPTA, Physics Department, Faculty of Science University Sidi Mohmmed ben Abdelah, Fes, Morocco
*Corresponding author E-mail: elbasset.abdelhalim@gmail.com

http://dx.doi.org/10.13005/ojc/320641

(Received: September 01, 2016; Accepted: October 03, 2016)

ABSTRACT

A series of new type of lead-free ceramics $Ba_{0.095}Be_{0.05}Ti_{1-x}Zr_xO_3$ (BBTZx) were prepared using the sol-gel method. X-ray diffraction results show that all powders crystallize in a perovskite-type phase, with the diffraction peaks of the $BBTZ_x$ powders shifting toward the smaller 2θ with increasing Zr content. On the other hand secondary phases (ZrO_2) were not detected in the diffractograms and the results of fluorescence spectroscopy measurements showed an increase in atomic percent of zirconium and a decrease of that of titanium, showing the incorporation of Zr ions in the BBT in place of Ti ones. The phase transition from tetragonal to cubic phase (T–C) was determined with the help of a new method based on the study of the thermal behavior of Cole-Cole diagrams (ε" vs ε').

Keywords: Ceramics $Ba_{0.095}Be_{0.05}Ti_{1-x}Zr_xO_3$, Dielectric, Cole-Cole diagrams (ε" vs ε'), Curie temperature (Tc).

INTRODUCTION

Since the discovery of the phenomenon of ferroelectricity, barium titanate $BaTiO_3$ was a standard material of the ferroelectric perovskite family. This compound has long been used in many industrial sectors such as electromechanical, the electronic and microwave applications[1,2] and electro-optical devices[3]. One of them, booming, is that of Multilayer Ceramic Capacitors MLCCs (Multilayer Ceramic Capacitors)[4-11]. An interesting and very current application of $BaTiO_3$ also relates to making computer memory frams (Ferroelectric Random Access Memories)[12], the detection of polluting gases such as CO[13] the optical waveguides, and holographic storage high frequency filters ...)[14-17]0 and the spatial light modulators[18]. This pure lead-free material and also strontium-doped, has a high environmental interest for applications mentioned above, due to its high dielectric constant value

combined with relatively low voltage dissipation and wide tunability of the dielectric constant, as well as a good chemical stability[19-21]. Several studies have examined the effect of doping on the dielectric properties and relaxer behavior, in particular doping with Zr (BZT) and Sr (BSTZ)[22-24]. Recently, we investigated the effect of substitution of Zr in the Ti site ($BaZr_xTi_{1-x}O_3$) and reported the diffuse behavior in BZT (for x> 0.1)[25]. Therefore, it would be interesting to study the effect of the substitution of Ti by Zr in other systems (nephews) as (($Ba_{0.95}Be_{0.05}$) ($Ti_{1-x}Zr_x$) O_3) ($BBTZ_x$). Thus, one aim of this work is the study of structural and dielectric properties of $BBTZ_x$ ceramics; in particular, in this work, the attention has been focused on the evolution of the Cole-Cole diagram (ε" vs ε') depending on the temperature of measurement.

EXPERIMENTAL AND METHODS

BBTZx ceramics samples with x = 0.075, 0.1, and 0.15 were prepared by the sol-gel method, using stoichiometric proportions of acetates of high purity: barium acetate ($Ba(CH_3CO_2)_2$; $3H_2O$, purity 99:9%, Johnson Matthey GmbH Alfa, Karlsrube, Germany), beryllium acetate ($C_{12}H_{18}Be_4O_{13}$), zirconium acetate ($Zr(CH_3CO_2)_4$; xH_2O) (purity 99.9%, x = 1.5, Johnson Matthey GmbH Alfa, Karlsrube, Germany), and titanium alcoxide (97 % (Assay) Johnson Matthey GmbH Alfa, Karlsrube, Germany). Appropriate quantities of these precursors were thoroughly mixed in a woodshed, under continuous agitation at 60°C. And then calcined at 1273 K under an air atmosphere for 4 h, and then pressed into pellets of 12 mm diameter and approximately 1 mm thickness, under a uniaxial pressure of 10 ton. The pellets were then sintered at 1472 K for 8 h in air. Steps of the preparation of BT and BZT have been detailed elsewhere[25-26]. Phase identification of the samples was performed using X ray diffraction (Cu K ray, λ = 1.5418 Å). However to verify the stoichiometry of our samples, we used fluorescence spectroscopy technique. Dielectric measurements were carried out in the frequency range of 100 Hz to 2 MHz using an inductance capacitance resistance (LCR) bridge (HP, Model 4284 A).

Table 1: Lattice parameters a, 2θ of (111) peak and strain values of $BBTZ_x$

Composition	2θ of (111) peak(°)	strain
BBT	38,3133	-0,99662
$BBTZ_{7.5}$	38,2103	0,92744
BBT_{10}	38,1763	0,93931
BBTZ15	38,1253	0,96327

RESULTS AND DISCUSSION

Fig.1 shows XRD spectra of the $BBTZ_x$ powders calcined at 1000 °C for 4 hours for different rates of Zr. It is observed that all powders crystallize in the perovskite phase with the presence of secondary microphase ($BaCO_3$); peaks associated with ZrO_2 (secondary phase) are not detected, indicating a complete incorporation of Zr ions into BT matrix. For x = 0 (Fig.1b) the presence of the peaks (200) and (002) is characteristic of the tetragonal phase 27),

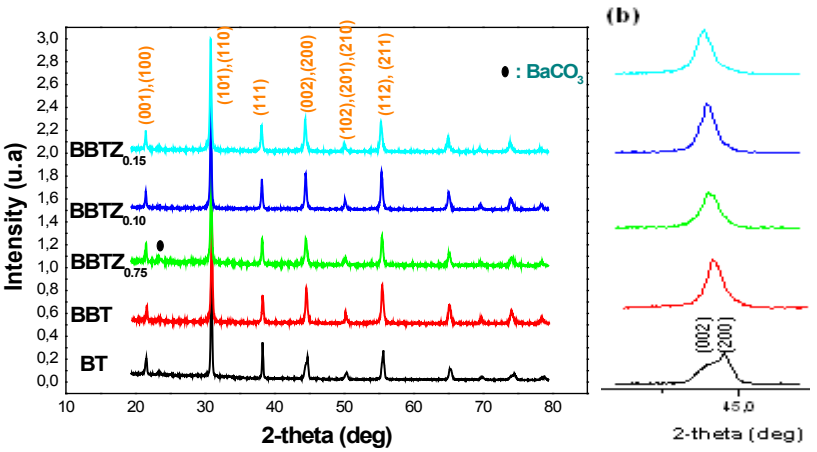

Fig. 1: XRD patterns of the powders $BBTZ_x$ calcined at 1000 °C

and with increasing Zr content they merge into one relatively large peak, which indicates a transition to the pseudo-cubic phase Moreover, a closer examination reveals that the increase in Zr content causes a displacement of the position of the peaks towards lower angles; the corresponding values of the 2θ position of the peak (111) of $BBTZ_x$ are given in table.1. This progressive displacement is attributed to the distortion (expansion) of $BBTZ_x$ crystalline structure with increasing Zr rate due to the fact that the ionic radii of Zr^{4+} (0.72 Å) is larger than that of Ti^{4+} (0.605 Å).

Fig. 2 shows the plot of β cos θ as a function of sinθ for different percentages of Zr in BBT. A linear fit to these points gives an estimate of the nature of stress in these compounds. For BBT powders (without Zr) a linear fit (Fig.2) shows a negative slope whereas for BBTZx powders, it becomes positive. It is also found that the slope (positive) increases, which means an increase of the tensile stress in the $BBTZ_x$ powders with increasing Zr content. However, for pure BBT powders (without Zr), the Be ion incorporation into the Ba sites creates a compressive stress due to smaller ionic radii of Be2 + ions (0.45 Å) with respect to that Ba^{2+} ions (1.35Å).

Results obtained from measurements using fluorescence spectroscopy technique are gathered in Table.2 showing an increase in atomic percent of zirconium and a decrease of that of titanium, pointing out a complete incorporation of Zr ions in place of Ti (B site in ABO_3 struture) ones in accordance of XRD results.

Fig. 3 displays Cole-Cole plots (from 1 kHz to 2 MHz) of the $BBTZ_x$ samples at different temperatures. These Cole-Cole diagrams show depressed observed semicircles With their center lying below the real impedance axis reveal a non Debye relaxation behavior with distributed relaxation time. This non-ideal behavior may be correlated to

Table 2: The percentage of chemical elements obtained by fluorescence spectroscopy of $BBTZ_x$ and εmax and T_c.

Composition	Ba	Be	Ti	O	Zr	εmax	T_c(°C)
BT	36,42	0	35,57	28,01	0	6048	130
BBT	36,12	0.31	35,57	28,01	0	5599	125
$BBTZ_{0.75}$	36,12	0.32	35,16	28,1	0,21	5402	110
$BBTZ_{0.10}$	36,11	0.31	34,41	28,19	0,98	4682	100
$BBTZ_{0.15}$	36,12	0.32	33,18	28,19	2,19	2633	80

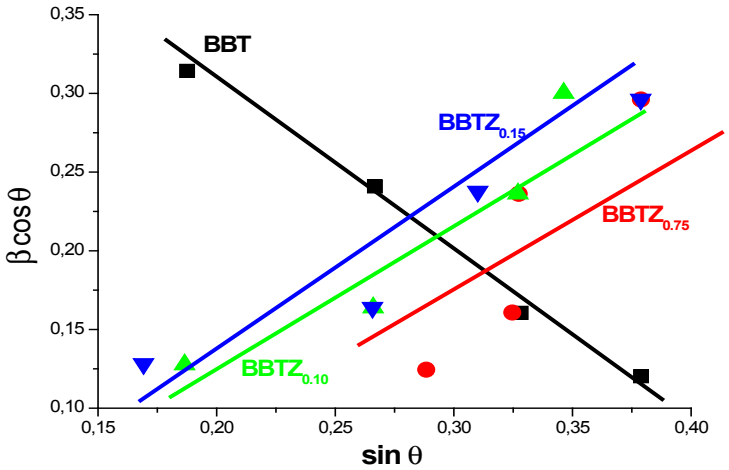

Fig. 2: Contraint curve of $BBTZ_x$ with different Zr contents.

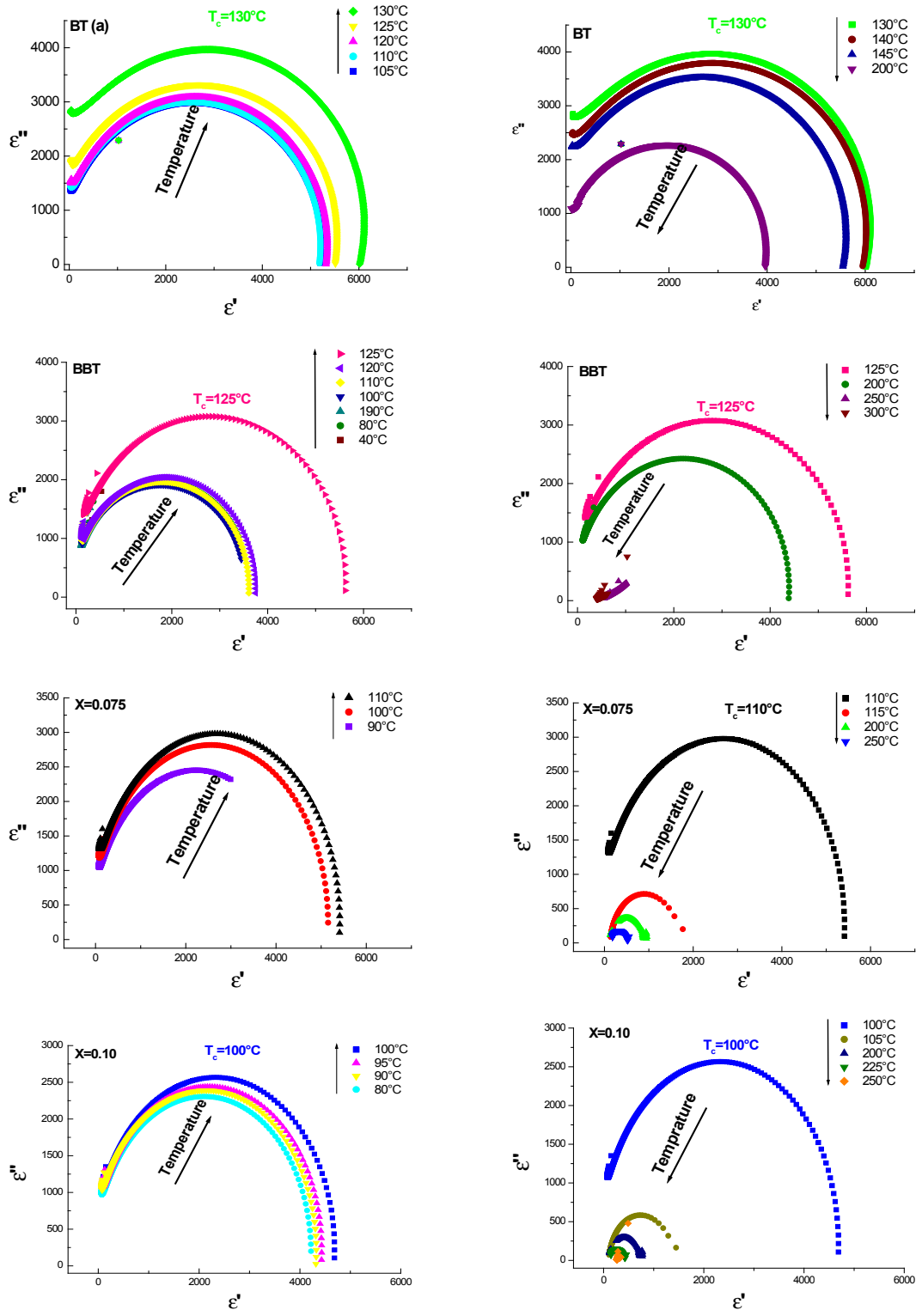

Fig. 3: Cole–Cole plot (ε"vs. ε') of different samples BBTZ$_x$ at different temperatures.

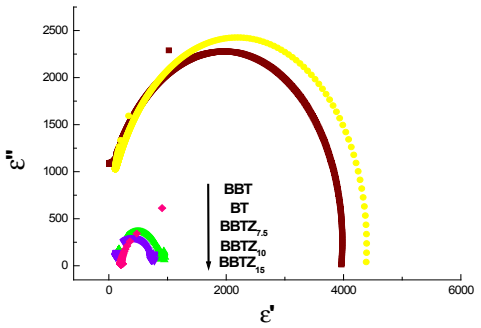

Fig. 4: Cole–Cole plot (ε"vs.ε') of different samples $BBTZ_x$ at 200°C.

several factors such as grain size distribution, grain orientation and grain boundaries. It can also be observed that for the temperature 200°C (fig.4) the plots are depressed semicircular in shape and their intercept on real axis shifts toward origin with increase in the rate of doping indicating the increase in the conductivity of the material. Moreover, substitution of Ti ions by Zr ones leads to distortions in the $BBTZ_x$ structure. The literature reports that the ionic radius of Ba^{2+} ions is about 1.34 nm, while that of Zr^{4+} is 0.72 nm. According to this hypothesis, the substitution of Ti sites, often occupied by atoms of Zr, causes electronic compensation through the formation of barium gaps or oxygen which causes a decrease of the dielectric constant what is clear in table.2.

Moreover, for pure BT, and for temperatures below 130°C (Fig. 3. a), one can notice that the half-circles have an increasingly large diameter with increasing temperature. This tendency is however inverted above 130°C (Fig. 3.b). According to the literature[28–31], this temperature (130°C), corresponds to the temperature of transition, Tc, from ferro-to-paraelectric phase. This observation is also valid for the other compounds at different concentrations in Zr. This result, which has never been reported in the literature, is observed due to the frequency measurement method, allowing determination of the transition temperature Tc without using other conventional methods consisting in collecting data for few frequency values which may prevent from observation of certain effects or phenomena.

CONCLUSIONS

Pure and Zr-doped BBT ceramics were successfully prepared. XRD patterns Rietveld refinement revealed that these powders crystallize in the perovskite phase at room temperature. Dielectric measurements show that the temperature Tc and the dielectric constant decrease with increasing doping either by Be or Zr. Evolution of Cole-Cole diagrams (ε" vs ε') revealed a non Debye relaxation behavior with distributed relaxation time. In this study we have given a new method to determine the fero-to-paraelectric temperature of transistion (Tc) based on the study of the thermal evolution of Cole-Cole diagrams (ε" vs ε').

REFERENCES

1. Cross, L.E.; *Mater. Chem. Phys*, **1996**, *43*, 108.
2. Hiroshi, M.; *Jpn. J. Appl. Phys*, **2007**, *46,* 7013.
3. Badapanda, T.; Panigrahi, S.; Rout, S.K.; Sinha, T.P.; Woo, S.I.; *J. Korean Phys. Soc*, **200**9, *55*, 749.
4. Wereszczak, A. A.; Breder, K.; Ferber, M. K.; Bridge, R. J.; Riester, L.; And Kirkland, T. P.; *American Ceramic Society, Cincinnati, Oh*, **1998** .
5. Shin, Y. I.; Kang, K. M.; Jung, Y. G.; Yeo, J. G., Lee; S. G., Paik, U.; *J. Euro. Ceram. Soc,* **2003**, *23*, 1427.
6. Nakano, Y.; Nomura T.; And Takenaka, T.; *Key Engineering Materials* **2003**, *248,* 179.
7. Yoon, D. H.; Lee, B. I.*; J. Euro. Ceram. Soc*, **2004**,.*24,* 753
8. Yokoi, H.; Wakiya, N.; Shinozaki, K; And Mizutani, N.; Key Engineering Materials, **2004**, *269*, 229.
9. Taïbi-Benziada, L.; Materials Science Forum, **2005**, *492*- 493, 109
10. Park, D. H.; Jung, Y. G.; Paik, U.; Ceramics International, **2005**, *31*, 655
11. Scott, J. F.; *Materials Science And Engineering B: Solid-State Materials For Advanced Technology*, **2005**, *120* (1-3), 6

12. Zhou, D.; Chen, Y.; Zhang, D.; Liu, H.; Hu, Y.; Gong, S.; *Sensors And Actuators* A, **2004**, *116*, 450.
13. Zhou, Z. G.; Tang , Z. L.; And Zhang, Z. T.; *Key Engineering Materials.* **2005**, *369,* 280
14. Iijima, K.; Tomita, Y.; Takayama, R.; and Veda, I.*; J. Appl. Phys*, **1986**, *60*, 361.
15. Okada, M.; Takai, S.; Ameniyer, M.; Tominaya, K.; *Jpn. J. Appl. Phys*, **1989**, *28*, 1030.
16. Li, A.H.; Zheng, Z.R.; Lü, Q.; Sun, L.; Xu, Y.H.; Liu, W.L.; Wu, W.Z.; Yang, Y.Q.; Lü, T.Q.; *J. Appl. Phys*, **2008**, *104,* 063526.
17. Mccaughan, L.; Gill D.M.; *US Patent*, **1993***, 5,* 227.
18. Ishida, M.. Matsunami H.; and Tanaka, T.. *Appl. Phys. Lett*, **1977**, *31*, 433.
19. Yu, Z.. Guo, R.. Bhalla, A.S.. *J. Appl. Phys*, **2000**, *88*, 410.
20. Zhao, J.; Li, L.; Wang, Y.; Gui, Z.; *Mater. Sci. Eng. B,* **2003**, *99,* 207.
21. Stojanovic, B.D.; Foschini, C.R.; Pavlovic, V.B.; Pablovic, V.M.; Pejovic, V.; J.A. Varela, *Ceram, Int*, **2002**, *28*, 293.
22. Maiti, T.; Guo, R.; Bhalla, A.S.; J. Phys. D*: Appl. Phys*, **2007**, *40*, 4355.
23. Kavita, V.; Seema, S.; *Ceramics International*, **2012**, *38*, 5957.
24. Yanhua, F.; Shuhui, Y.; Rong. S.; Lei. L.; Yansheng. Y.; , Ruxu. D.; *Thin Solid Films*, **2010**, *518*,3610 .
25. Elbasset, A.; Abdi, F.; Lamcharfi, T.; Sayouri, S.; Abarkan, M.; Echatoui and, N. S.; Aillerie**,** M.; *Indian Journal of Science and Technology*, **2015***, 8*(13)*,* 56574.
26. Elbasset, A.; Sayouri , S.; *Adv. Mater. Lett*, **2015**, *6*(11), 999.
27. Zhang, J.; Zhai, J.; Chou, X.; Shao, J.; Lu, X.; Yao, X.; *Acta Materialia*, **2009**, *57,* 4491.
28. Kim, S.W.. Choi, H.I.; Lee, M.H.; Park, J.S.; Kim, D.J.; Do, D.; Kim, M.H.; Song, T.K.; Kim, W.J.; *Ceramics International*, **201**3*, 39,* S487.
29. Darwish, A.G.A.. Badr, Y.. El Shaarawy, M.. Shash, N.M.H.. Battisha, I.K.. *J. Alloys Compd.* **2010**, *489*, 451.
30. Horchidan, N.; Ianculescu, A. C.; Curecheriu, L. P.; Tudorache, F.; Musteata, V.; Stoleriu, S.; Dragan, N.; Crisan, D.; Tascu, S.; Mitoseriu, L.; *J. Alloys Compd*, **2011***, 509*, 4731.
31. Kavian, R.; Saidi, A.; *J. Alloys Compd*, **2009**, *468*, 528.